Climate Dynamics (2005) 25: 537–553
DOI 10.1007/s00382-005-0053-0

G. van der Schrier · J. Barkmeijer

Bjerknes' hypothesis on the coldness during AD 1790–1820 revisited

Received: 1 July 2004 / Accepted: 16 November 2004 / Published online: 17 August 2005

Abstract The aim of this paper is to re-examine and quantify a hypothesis first put forward by J. Bjerknes concerning the anomalous coldness during the AD 1790–1820 period in western Europe. Central to Bjerknes' hypothesis is an anomalous interaction between ocean and atmosphere studied here using an ocean-atmosphere coupled climate model of intermediate complexity. A reconstruction of the sea-level pressure pattern over the North Atlantic sector averaged over the period 1790–1820 is assimilated in this model, using a recently developed technique which has not been applied to paleoclimatic modelling before. This technique ensures that *averaged* over the simulation the reconstructed pattern is retrieved whilst leaving atmospheric and climatic variability to develop freely. In accordance with Bjerknes' hypothesis, the model results show anomalous southward advection of polar waters into the north-eastern North Atlantic in the winter season, lowering the sea-surface temperatures (SSTs) there with 0.3–1.0°C. This SST anomaly is persistent into the summer season. A decrease in western European winter surface air temperatures is found which can be related almost completely to advection of cold polar air. The decrease in summer surface air temperatures is related to a combination of low SSTs and anomalous atmospheric circulation. The modelled winter and summer temperatures in Europe compare favourably with reconstructed temperatures. Enhanced baroclinicity at the Atlantic seaboard and over Baffin Island is observed along with more variability in the position of the North Atlantic storm tracks. The zone of peak winter storm frequency is drawn to the European mid-latitudes.

In the original article (Climate Dynamics (2005) 24: 355-371; http://dx.doi.org/10.1007/s00382-004-0506-x) figures 4, 7, 8, 10, 11 and 13 were unfortunately incorrect. The correct version is shown here.

G. van der Schrier (✉)
Climatic Research Unit, UEA, Norwich, NR4 7TJ, UK
E-mail: g.schrier@uea.ac.uk
Tel.: +44-1603-592318

J. Barkmeijer
Royal Netherlands Meteorological Institute (KNMI),
De Bilt, NL

Introduction

Recent studies (IPCC 2001; Crowley 2000) indicate that as much as 41–64% of pre-1850 Northern Hemisphere averaged temperature variations on decadal timescales is related to changes in solar activity and volcanism, while the late twentieth century warming closely agrees with the response predicted from greenhouse gas forcing. Additionally, compilations of historic data and documentary evidence show that on a *regional* scale, decadal climate variations in the Atlantic sector have been even more profound over the past ca. 500 years which was a period in Europe punctuated by short intervals with harsh winters and generally cooler summers (Luterbacher et al. 2004).

One of these anomalously cold intervals is the so-called Dalton Minimum (Grove 1988), ca. AD 1790–1830. During this period sustained low solar activity was observed which accounts for its name. Moreover, two major explosive volcanic eruptions occurred during this period, one unknown at 1809 (Robertson et al. 2001) and the Tambora explosion in 1815 which preceded the well-known 'year without a summer' (Harington 1992). The Dalton Minimum in Europe also seems to be characterized by an anomalous atmospheric circulation (Luterbacher et al. 2002b). Overall, anomalously cold periods like the Dalton Minimum have given rise to changes in the Atlantic storm track and an increased storm intensity and/or frequency (Glaser 2001; Lamb 1985), and in oceanic conditions, like changes in sea-ice cover (Ogilvie and Jonsson 2001) and sea surface temperatures (Keigwin 1996; Keigwin and Pickart 1999).

There exists a large body of literature on the connection between past hemispheric and regional climate change and solar activity and explosive volcanic outbursts (Waple et al. 2002; Rind et al. 1999; Rind et al. 2004; Shindell et al. 2003; Shindell et al. 2004; Zorita et al. 2004) which study this relation both from the modelling and the observational perspective. A recent study (Wagner and Zorita, submitted to Climate Dyn.) based on extensive modelling with a state-of-the-art general circulation model and aimed specifically at the Dalton Minimum, suggests that on global and hemispheric scales, the volcanic forcing is largely responsible for the temperature anomaly during this period. Changes in solar activity proved to be of less importance.

If the changes in Earth's radiation budget due to changes in solar activity and atmospheric dust loading are the primary causes for the coldness of the Dalton Minimum, as suggested above (IPCC 2001; Crowley 2000), its regional variation must then be caused by secondary effects. Studies like those of Shindell et al. (2001) and Haigh (1996) offer a framework in which the (zonally uniform) primary causes can be tied to regional variations in atmospheric circulation. This involves the impact of solar activity and volcanic dust loading on the stratospheric climate. Both these forcings create a stratospheric meridional temperature contrast, which feeds back on the stratospheric zonal circulation strength, via the thermal wind balance (Hartmann et al. 2000). Interaction between the tropospheric planetary wave propagation and the zonal wind anomaly in effect carry the zonal wind anomaly steadily downward from the stratosphere into the troposphere (Hartmann et al. 2000). This allows stratospheric changes to affect regional surface climate conditions by altering the tropospheric circulation. And indeed, Shindell et al. (2004) present evidence that a strong volcanic eruption does have an impact on modes of variability of the tropospheric circulation over the Atlantic sector.

The perspective of Bjerknes (1965), and the perspective we take in this study, is different from the above. Starting from a documented change in atmospheric circulation over the Atlantic sector, Bjerknes put forward the idea of anomalous ocean-atmosphere interaction in an attempt to point out the possible nature of these northwestern European cold climatic anomalies, leaving a possible connection to primary causes as volcanic dust loading and solar activity open.

In his study, Bjerknes viewed the period 1790–1829 as representative for the 'Little Ice Age', but a more modern view is that this term for the period ca. AD 1550–1850 does not reflect the highly complex and spatially rather inhomogeneous climate of that period (Jones and Mann 2004). We therefore simply use calendar dates or use the term 'Dalton Minimum', without implying that a minimum in solar activity was the ultimate cause of lowered temperatures during this period.

Bjerknes concluded that the period 1790–1829 was characterized by anomalous low pressure off the eastern seaboard of the US, extending roughly into the western Sargasso Sea, and anomalous high pressure in the central North Atlantic, just south off Iceland. This was based on the mean January sea level pressure (SLP) maps as reconstructed by Lamb and Johnson (1959). By using the Sverdrup relation (Pedlosky 1987), which relates meridional geostrophic water transport to the curl of the wind stress, Bjerknes related anomalous southward geostrophic flow in the Atlantic to the anomalous anti-cyclonic conditions and conversely, anomalous northward flow to the anomalous cyclonic conditions. The effect of the anomalous meridional geostrophic transports in the northeast Atlantic would then be less northward water transport, leaving the northeast Atlantic, North Sea and Norwegian Sea colder than at present. Furthermore, the change in geostrophic transport in the northeast Atlantic could have shifted in the position of the oceanic polar front to a more zonal orientation.

The anomalous northward geostrophic flow in the western Sargasso Sea could have relocated the center of the subtropical gyre somewhat further downstream along the Gulf Stream, bringing the point of maximum volume transport also somewhat downstream. This locally affects the oceanic heat transport, resulting in a warming of the western Sargasso Sea.

Bjerknes' hypothesis offers an explanation for lower than normal European winter and summer temperatures during the AD 1790–1829 period based on a reconstruction of atmospheric circulation for this period. The climatic situation hypothesized by Bjerknes in the North Atlantic gave rise to the situation that westerly winds advected anomalously cold air, having been in contact with the anomalously low temperatures in the waters west of the European continent. Bjerknes qualified this as 'probably the most important factor in maintaining the European Little Ice Age'. The repositioning of the polar front might also explain the advance of Arctic sea ice around Iceland (Jennings et al. 2001). Bjerknes noted that the increase in sea-surface temperatures (SST) in the western Sargasso Sea leads to favourable baroclinic conditions for frontal cyclogenesis along the Atlantic seaboard, offering an explanation of the possible changes in the Atlantic storm climate during cold periods like the Dalton Minimum.

In this study, we aim to quantify Bjerknes' hypothesis in a General Circulation Model of intermediate complexity. To achieve this, we first asses the validity of the averaged anomalous SLP patterns he used by comparing it with a recent reconstruction of SLP (Luterbacher et al. 2002) which has been extended to include the complete extra-tropical North Atlantic ocean and part of the northeastern USA. Secondly, we introduce and apply a data-assimilation technique not used in paleoclimatology before. The aim of an assimilation technique would be to construct a simulation of climate which is consistent with the reconstruction of atmospheric circulation. With the technique used in this study it is possible to make a simulation of global climate which on the one hand reproduces, in a time-averaged sense, the recon-

structed SLP field, while on the other hand leaving the atmosphere free to respond in a dynamically consistent way to any changes in climatic conditions. Importantly, synoptic-scale variability internal to the atmospheric or climatic system is not suppressed and can adjust to the changes in the large-scale atmospheric circulation. This yields a simulation of Dalton Minimum climate in the Atlantic sector which is consistent with the reconstruction of atmospheric circulation over this period. The emphasis of this study is strongly on the latter part. The SLP reconstruction relies heavily on previous work of Luterbacher et al. (2002) and Lamb and Johnson (1959) and is no more than a simple synthesis of these studies.

This study is organized as follows: in Sect. 2 the SLP reconstruction over the extra-tropical North Atlantic is computed and compared with an earlier reconstruction. Section 3 gives a short description of the model and in Sect. 4 an introduction to the data assimilation technique used in this study is given. Results are presented in Sect. 5 and the study is discussed in Sect. 6. Section 7 gives a summary and the conclusions.

Sea level pressure reconstruction

Recently, Luterbacher et al. (2002) reconstructed sea level pressure fields extending over a region from the eastern North Atlantic to Eastern Europe at 40°E back to AD 1500. This dataset consists of gridded monthly sea level pressure fields from 1659 to the present and is based on a combination of early instrumental station series (pressure, temperature, precipitation) and documentary evidence from Eurasian proxy data. The verification results from the twentieth century indicate that reconstruction of SLP has considerable skill, especially in winter and even at the fringes of the grid (Luterbacher et al. 2002).

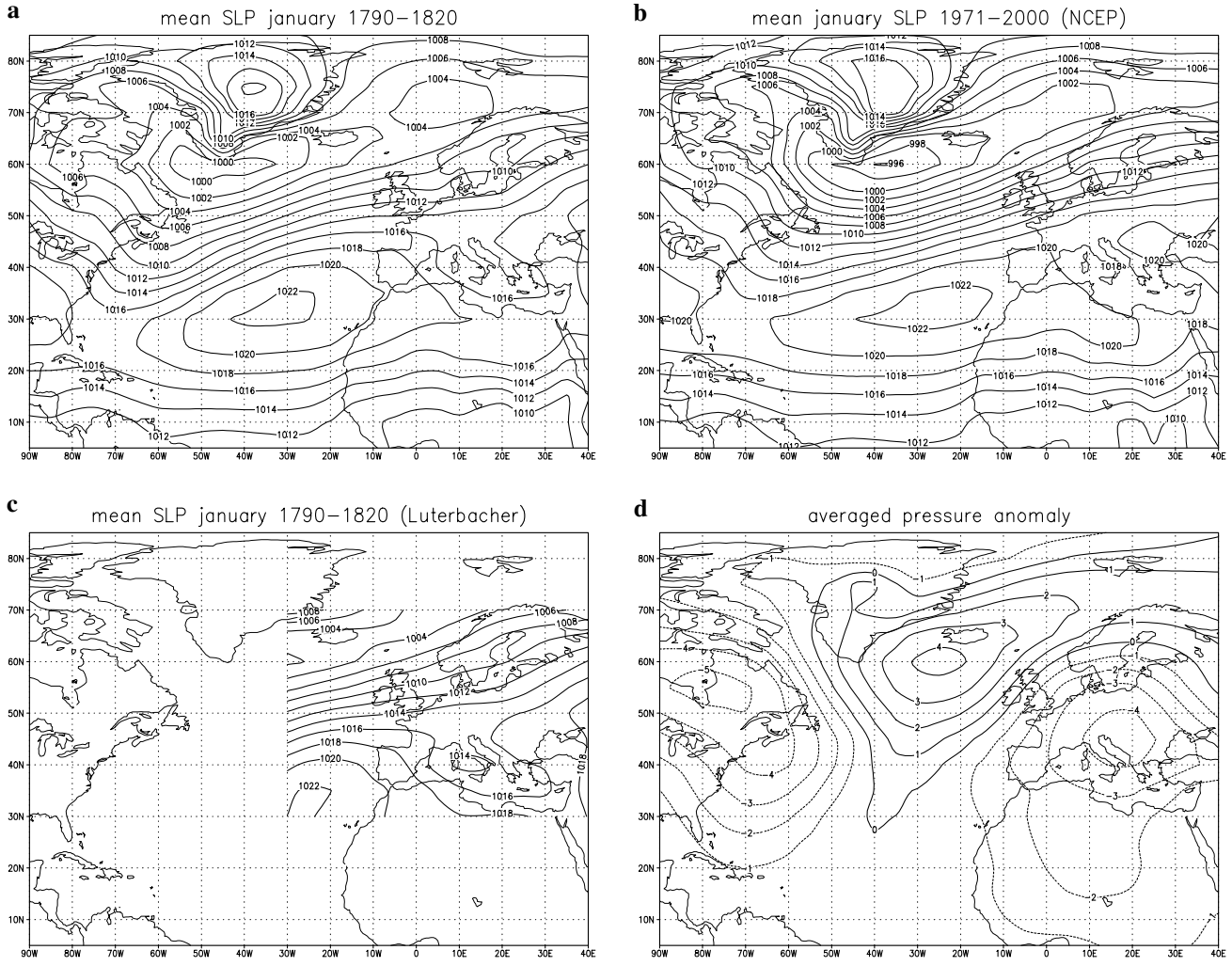

Fig. 1 The reconstructed January SLP pattern, averaged over the years 1790-1820 (fig. a), the averaged January NCEP SLP pattern averaged over 1971-2000 (b), the Luterbacher et al. (2002) reconstruction for this period (c) and the time averaged SLP anomaly pattern (fig. d)

An estimate of anomalous SLP during the Dalton Minimum is based on this dataset (covering the area 30°W–40°E, 30°N–70°N) and additional data from the US east coast. The latter are provided by a record of daily weather observations for Salem, Massachusetts, by Dr. Edward A. Holyoke (Hale 1833). These data, and others from the US dating from the mid-eighteenth to early nineteenth century were compiled by Havens (1956). Dr. Holyoke started his meteorological journal when he was over 50 years old and continued it until a few weeks before his death at age 100 in 1829. Apart from three daily temperature readings, he made two daily barometer readings at 8 a.m. and 10 p.m. Lamb and Johnson (1959) (LJ here after) qualify this record with the remark that it 'appears more homogeneous and trustworthy than that of most official observatories of that time.' The daily barometer readings are averaged to provide a monthly averaged atmospheric pressure dataset. After 1820, Dr. Holyoke continued his observations without the barometer readings. Consequently, we will focus on the 1790–1820 period, rather than the 1790–1829 period LJ used.

In order to compare the SLP reconstruction to that of LJ, who reconstruct January and July fields only, we focus on the January SLP reconstructions. In the following we take the January reconstruction to be representative for the DJF averaged SLP field.

To extend the Luterbacher et al. SLP reconstruction to the east and to the south, we used an empirical orthogonal functions (EOF) based method, which is shown to yield satisfactory results (Sterl 2001). The first N EOFs of the NCEP reanalysis January SLP dataset are computed over the spatial domain 90°W–40°E, 5°N–85°N, which includes the domain on which Luterbacher et al. reconstructed SLP and extents over the North Atlantic to include the US east coast. For each separate

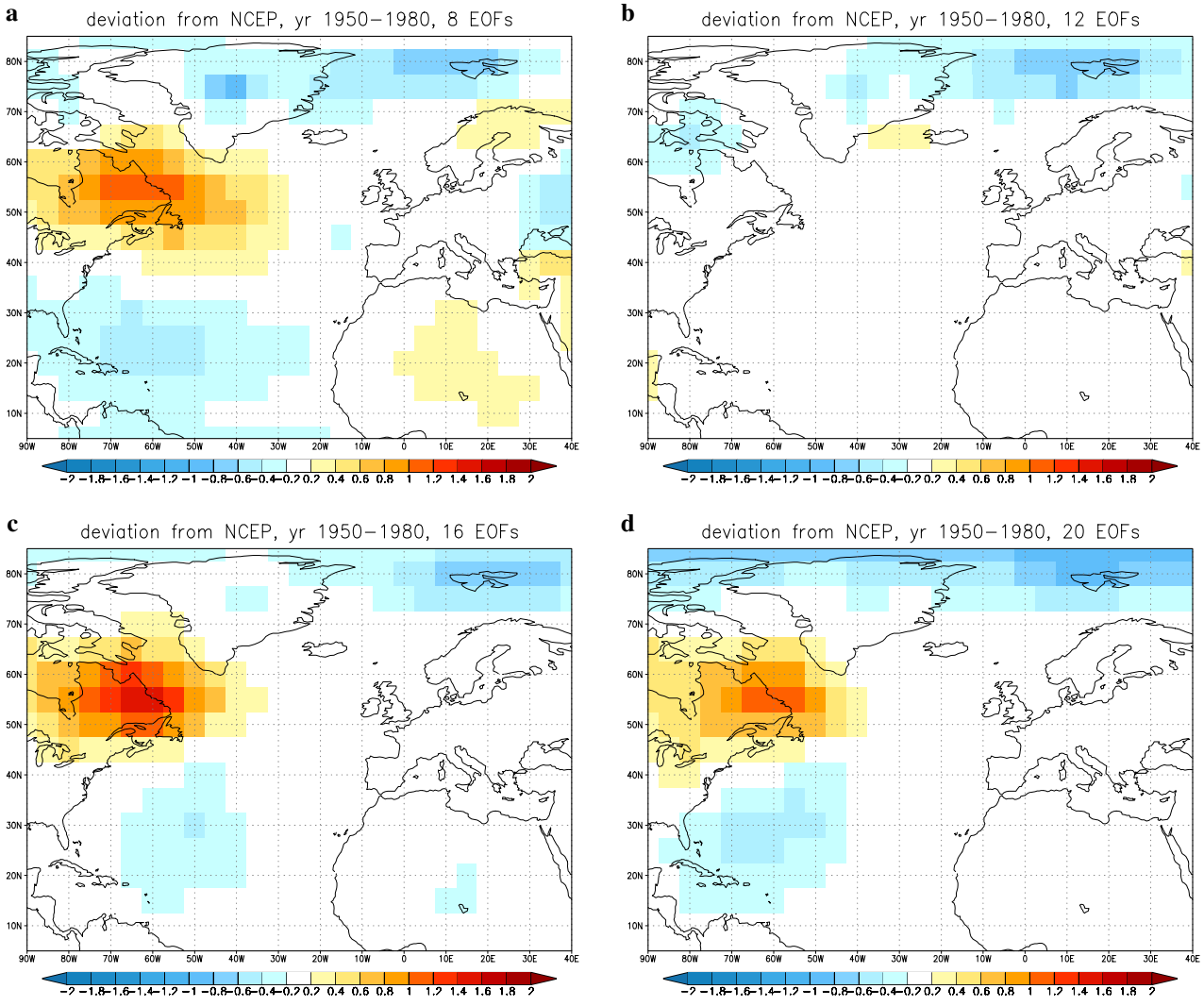

Fig. 2 Plots of the residual after applying the reconstruction technique to the NCEP reanalysis January SLP data for the years 1950-1980. The overall residual is lowest when the first 12 EOFs of NCEP January SLP are used (box b), and is $\approx \pm 0.4$ mbar. Although the residual in the training area 30°W-40°E, 30°N-70°N reduces when more EOFs are used, the residual in the remainder of the domain increases

year, the NCEP 1971–2000 January SLP climatology (Trenberth and Paolino 1980) is subtracted from Luterbacher et al.'s January SLP reconstruction and the January averaged atmospheric pressure in Salem, as given by the Holyoke record. This gives two disjunct anomalous SLP fields; one over Europe and one representative for Salem only. For every year separately, the set of EOFs is now multiply regressed upon the anomalous SLP fields such that, in a least-squares sense, the combination of EOFs explain optimally the anomalous SLP fields. Note that the regression is over the spatial dimension rather than the time dimension. Data from the Holyoke record was given a higher weight in the least-squares computation than the other data to counter-weight the abundance of data from the Luterbacher et al. reconstruction. A ten times higher weight proved sufficient to faithfully reflect the Holyoke record in the larger SLP reconstruction. This combination of EOFs closely resembles, by construction, the Luterbacher et al. reconstruction and the Holyoke data (Fig. 1).

To test the experimental set-up of this procedure and to determine an optimal value of N, we performed the following test. The first N EOFs of the January NCEP reanalysis computed over the larger domain (90°W–40°E, 5°N–85°N) were regressed over January SLP fields of the smaller domain (30°W–40°E, 30°N–70°N) of the same dataset. The time-averaged difference of the reconstruction produced in this way and the actual reanalysis data, the residual, is shown in Fig. 2 for four different values of N. It appears that the residual outside the smaller domain initially decreases but increases again when more EOFs are included. The smallest residual is obtained with 12 EOFs.

A comparison between the LJ and the Luterbacher et al. (2002) based reconstruction presented in this study shows similar features, giving further credit to the current reconstruction (Fig. 3). Some differences are that the Azores high, although located similarly, is more extensive in the current reconstruction and SLP in the western subtropical Atlantic is higher. The high pressure system over western Russia is lacking and SLP in the southern Greenland-Iceland-Norway (GIN) Sea seems to be slightly higher also.

Sea level pressure is not a prognostic variable in the model. To be able to apply the data-assimilation technique, we computed the geopotential height field at 800 hPa which is associated with the SLP reconstruction, and transformed this in the streamfunction Ψ. There is a linear transformation between the streamfunction and the model's prognostic variable potential vorticity.

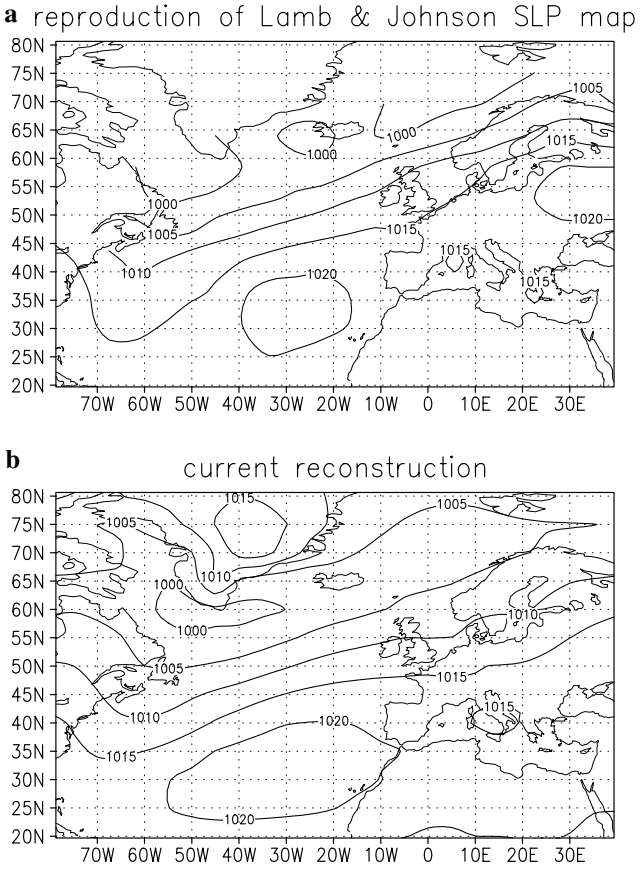

Fig. 3 A redrawn map of the reconstructed January SLP pattern for the period 1790-1829 as produced by Lamb & Johnson (1959) (fig. a) and the averaged January SLP pattern from the reconstruction, averaged over 1790-1820, based on the Luterbacher et al. (2002) reconstruction and the Holyoke data (fig. b)

Model description

The model, ECBilt-Clio, is a coupled ocean-atmosphere-sea ice general circulation model of intermediate complexity (Opsteegh et al. 1998; Goosse and Fichefet 1999). The atmospheric component (ECBilt) resolves 21 wavelengths around the globe. It has three levels in the vertical, at 800, 500 and 200 hPa. The dynamical part is an extended quasi-geostrophic model where the neglected ageostrophic terms are included in the vorticity and thermodynamic equations as a time dependent and spatially varying forcing. With this forcing the model simulates the Hadley circulation qualitatively correctly, and the strength and position of the jet stream and transient eddy activity become fairly realistic in comparison to other T21 models. The essentials of baroclinic instability are included, but the variability associated with it is underestimated compared to modern observations. The model contains simple physical parameterizations, including a full hydrological cycle. Cloud cover is prescribed following a seasonally and geographically distributed climatology (D2 monthly data set of the International Satellite Cloud Climatology Project).

The oceanic component (Clio) is a primitive equation, free-surface ocean general circulation model coupled to a thermodynamic-dynamic sea ice model and includes a relatively sophisticated parametrization of vertical mix-

ing (Goosse et al. 1999). A three-layer sea-ice model, which takes into account sensible and latent heat storage in the snow-ice system, simulates the changes of snow and ice thickness in response to surface and bottom heat fluxes. The horizontal resolution of Clio is $3° \times 3°$ and it has 20 unevenly spaced layers in the vertical. To avoid the singularity of the lat-lon grid at the North pole, Clio has in the North Atlantic and Arctic ocean a rotated grid, with poles located at the equator in the Pacific and Indian ocean.

The ECBilt model has been used in several paleoclimatic modelling studies before, focusing on late-Holocene sea-level variability (van der Schrier et al. 2002; van de Plassche et al. 2003) or on responses internal to the climate system to the documented changes in Holocene irradiance forcing (Weber et al. 2004).

The data-assimilation technique

Data assimilation (abbreviated by DA hereafter) techniques which have been developed in operational meteorology are intended to force the model state toward the observed field. This is done in operational weather forecasting by constructing an initial condition which leads after a short integration to the observed field. For every new forecast, a new initial condition needs to be computed. This technique requires very detailed knowledge of the atmospheric state, till at the level of the smallest spatially resolved scales and at a temporal scale of days. In paleoclimatology, this precise knowledge of the past atmospheric state is absent, where one typically has proxy or documentary data from a few locations, often reflecting climate signals that are integrated over weeks or months (or longer). This renders the traditional DA techniques in paleoclimatology useless.

Here we apply a technique, recently developed at the European Centre for Medium Range Weather Forecasts (ECMWF), which can be used to overcome this problem. This technique determines small perturbations to the time evolution of the prognostic variables (the tendencies) which optimally lead the atmospheric model to a pre-defined target pattern. These tendency perturbations are referred to as *forcing singular vectors* (Barkmeijer et al. 2003) and can be computed using a so-called adjoint model (Lacarra and Talagrand 1988).

The forcing singular vectors have amplitudes which are typically less than 1% of the total tendencies and are used to modify large-scale patterns of variability only, leaving the synoptic scale variability to evolve freely. A detailed description of forcing singular vectors and their computation is given by Barkmeijer et al. (2003) and in the Appendix to this paper. In this section we give a brief outline only.

We are interested in tendency perturbations, **f**, that will produce, after some integration time, or an optimization time, a deflection of the model atmospheric state in the direction of the target pattern. The amplitude of this deflection is $1 - \alpha$ times the amplitude of the target pattern, where α is the projection coefficient of the model atmosphere on the target pattern.

If the tendency perturbations are sufficiently small, the evolution of deviations of the model atmospheric state which results from tendency perturbations can be computed by a linearization of the GCM along a (time-dependent) solution of this GCM. Thus the linear evolution of a perturbation ε, measuring the deviation between a control and perturbed model run, satisfies:

$$\frac{d\varepsilon}{dt} = \mathbf{L}\varepsilon + f, \tag{1}$$

where **L** is the time dependent linearization of the GCM along a solution. For a forcing perturbation **f**, the vector $\varepsilon(t = T) \equiv \mathscr{M}\mathbf{f}$ is simply determined by integrating Eq. 1 to time $t = T$ with initial condition ε $(t = 0) = 0$. The forcing perturbation is now determined by minimization of:

$$\left| P\left(\mathscr{M}\mathbf{f} - (1 - \alpha)\psi_{\text{target}} \right) \right| \tag{2}$$

where ψ_{target} is the target pattern in streamfunction and P is a projection operator onto the 800 hPa level over the extra-tropical North Atlantic sector. The atmospheric state *outside* the North Atlantic sector, north of the subtropics, and on the levels higher than 800 hPa does not enter in the cost function. The norm used here to constrain **f** is a simple L_2-norm, but other norms can be used too. A fast and efficient minimization routine requires the derivative of Eq. 2 with respect to **f**, which can be efficiently computed using the adjoint of $\mathscr{M}$.

A linearization of the atmospheric part (ECBilt) dynamic core of the climate model and its adjoint exist. They have been used earlier in predictability studies, e.g. Barkmeijer et al. (1993) and are used here too in the evaluation of the forcing perturbation **f**. Atmospheric physics is not included in the computation of **f**; an accurate approximation if the optimization time T is sufficiently small.

The choice for the optimization time T is based on the following considerations. When T is too small, say 12 h, **f** is no longer small compared to the internal forcings. In that case the optimization time is simply too short for a small but persistent forcing to have a large impact on the atmospheric dynamics. When T is too large, say 240 h, the accumulated effect of atmospheric physics on the streamfunction are large enough to violate the assumption that the atmosphere only evolves according to atmospheric dynamics. The optimization time is chosen between these bounds as a requirement to keep the tendency perturbation as small as possible and the need to faithfully reproduce the target pattern. For instance, when T is chosen as 168 h, then the streamfunction will reflect the target pattern only once every week. On the remaining days this need not be the case due to the effects of internal variability which blurs the similarity

between the target pattern and the simulation. On the other hand, updating the tendency perturbation too frequently may result in the situation where the model atmospheric state does not have the chance to deviate significantly from the target pattern.

In this study, the optimization time T has been set to 96 h, which means that every 96 h $\mathbf{f}$ is updated. This proved long enough not to affect the overall level of atmospheric variability in the North Atlantic sector while still being short enough not to violate the assumption that the impact of atmospheric physics was not too large. This value was arrived at on the basis of a number of short test simulations.

The approach used in this study has the same aim as the pattern nudging method of the Data Assimilation Through Upscaling and Nudging (DATUN) initiative (von Storch et al. 2000; Jones and Widmann 2004), although the approach in this latter technique is very different from the one introduced above. There are some potential advantages of computing the singular forcing vectors as a perturbation to the tendencies rather than computing an additional artificial forcing for the tendencies with a nudging method. One is that the latter method, as with all traditional nudging techniques, the model atmosphere is changed such that the intensity of the target pattern is brought toward its prescribes target intensity at every timestep; effectively suppressing variability in this particular pattern. The current technique forces the model to make after every optimization time T at a single timestep, a realization of the target pattern. It does not constrain the intensity of the target pattern at the other timesteps during the optimization time. A disadvantage of the current method is the requirement of an adjoint model, making the DATUN approach more generally applicable.

Results

A 25-year simulation was made where, only during the DJF season, tendency perturbations are computed which force the 800 hPa Ψ field toward the reconstructed field. No tendency perturbations are added in the remaining months of the year. The reason for this being that Bjerknes' theory relates only to the winter climate. This simulation is referred to as the data-assimilated (DA) simulation. In addition, a 50-year control run is made in which the DA technique is disabled.

The forcing of the ECBilt model at the top of the atmosphere is constant and equal for the control simulation and the DA simulation. No attempt is made to parameterize the effects of changes in volcanic dust loading or solar activity as they have occurred during the Dalton Minimum period through a change in total solar irradiance.

The initial conditions for both the model atmosphere and ocean for the control and the DA simulations are identical. Any changes between the DA and the control simulation arise through the data-assimilation in the model atmosphere only. Consequently, any changes in the model's oceanic climate are initially slaved to changes in the model atmosphere through changes in the ocean-atmosphere heat and momentum fluxes. However, the changes in the oceanic climate can feed back on the atmosphere (as is possible with all coupled ocean-atmosphere models).

No changes in the model vegetation cover between the control and the DA simulation exist.

Atmospheric circulation

The difference streamfunction Ψ between the DA and control simulation is shown in Fig. 4b (averaged over 25 years, DJF season shown), with the target pattern shown in Fig. 4a. The strength and position of the anomalous minima and maxima over Labrador and Iceland are reasonably well reproduced. The anomalous minimum over the European continent, although weakly present, fails to be well developed. However, when the

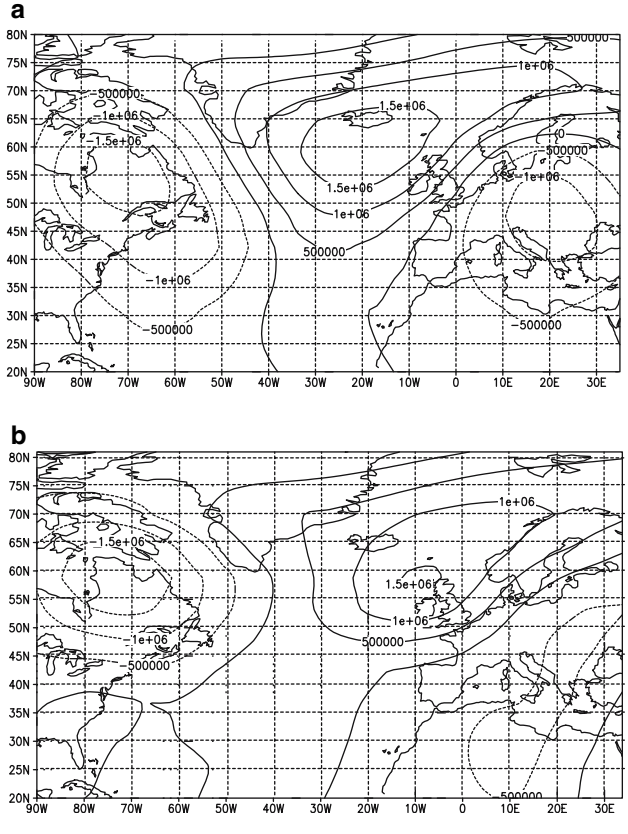

Fig. 4 Anomalous streamfunction Ψ in $m^2\ s^{-1}$ which was used in the data-assimilation simulation (fig. a) and the difference in Ψ (DJF) between the data-assimilated run and the control run, averaged over the length of the data-assimilated simulation. The strength and position of the anomalous low and high over Labrador and Iceland are reasonably well reproduced. The anomalous low over the European continent is not reproduced

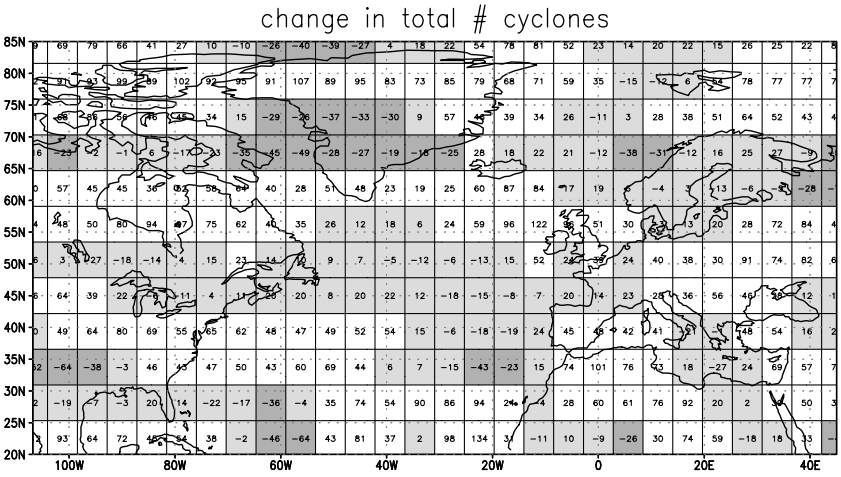

Fig. 5 Differences in the number of cyclones for each gridbox (DJF season only), between the data-assimilated and the control simulations. Areas of increasing cyclone activity are white. Areas with decreasing or unchanging cyclone activity are dark grey. Changes in the light grey areas are not significant at the 95% level

DJF averaged, year-to-year Ψ field is monitored (not shown), a distinct minimum over Central Europe is frequently observed. The randomness of atmospheric internal variability prevents a clear minimum to show up in the 25-year averaged field.

In order to asses the North Atlantic storm track response, 4-hourly relative vorticity ζ over the North Atlantic sector is analyzed, where, following the suggestion of Hoskins and Hodges (2002), the planetary scales with total wavenumber less than or equal to five are removed from every field at each timestep. This removal of the background system highlights the synoptic system.

Figure 5 shows the change in the total number of cyclones between the DA simulation and the control run for each gridbox in the Atlantic sector. Data are from the DJF season only. In this analysis a 'cyclone' ('anticyclone') is characterized as having a relative vorticity which is lower (higher) than minus (plus) the standard deviation and is lower (higher) than the relative vorticity of neighbouring gridboxes. The standard deviation used here is that of the gridbox with the largest variability. From this it is evident that along the eastern seaboard of the US the change in atmospheric circulation has led to an increase in cyclonic frequency in a narrow zone extending from southeastern Canada to the British Isles and in a broader zone from the mid-west into the mid-Atlantic ocean. These bands are situated north and south of the control run's storm track, indicating more variability in the position of individual storm tracks, leading to a broadening of the storm track and a southward shift. As Fig. 5 shows, the change in cyclone frequency was largest at the southern Atlantic coast near 40°N. On the northern edge of the control run's storm track a band of increased cyclonic activity is seen too, extending from south Canada, over the Hudson Bay into the Atlantic. The largest increase in cyclone activity in this band is found northwest of Ireland.

Along with changes in the position of the storm track in the data assimilated simulation, a change in the strength of the cyclones is observed. The probability distribution of the relative vorticity ζ is computed for the gridboxes at 800 hPa in the area bounded by 20°W–1°E and 47.8°N–64.7°N (12 gridboxes located at the European mid-latitudes), for both the control and the DA simulation. The probability distribution for these gridboxes (Fig. 6) shows a higher frequency for the most negative values in ζ compared to that of the control simulation. Both distributions have been smoothed by a 11-point Gaussian smoother, and the difference between the two distributions is highly significant according to a standard Chi-square test (probability 2.5×10^{-33}). The change in probability distribution under 'Dalton Minimum' conditions for ζ averaged over this region indicates that at these latitudes storm activity is higher than in the control run. Also, the severest storms occur in the DA simulation more frequently than in the control run. Conversely, positive values in ζ at this latitude in the DA simulation have a lower probability than that in the control run. This situation is reversed for more northerly latitudes where the maxima in ζ are stronger and more

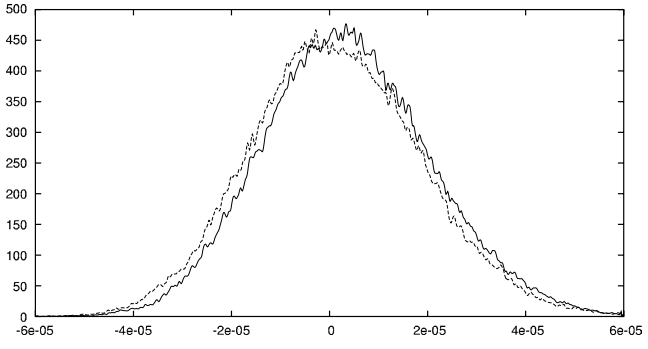

Fig. 6 Probability distribution (smoothed by a 11-point Gaussian smoother) of relative vorticity ζ in the area bounded by 20°W-1°E and 47.8°N-64.7°N (12 gridboxes) at 800 hPa for the control run and the data-assimilated simulation (solid and dashed respectively). The data-assimilated simulation shows a probability distribution which is shifted to more negative values for ζ compared to that of the control run. This indicates a higher probability of occurrence of strong cyclones in the European mid-latitudes

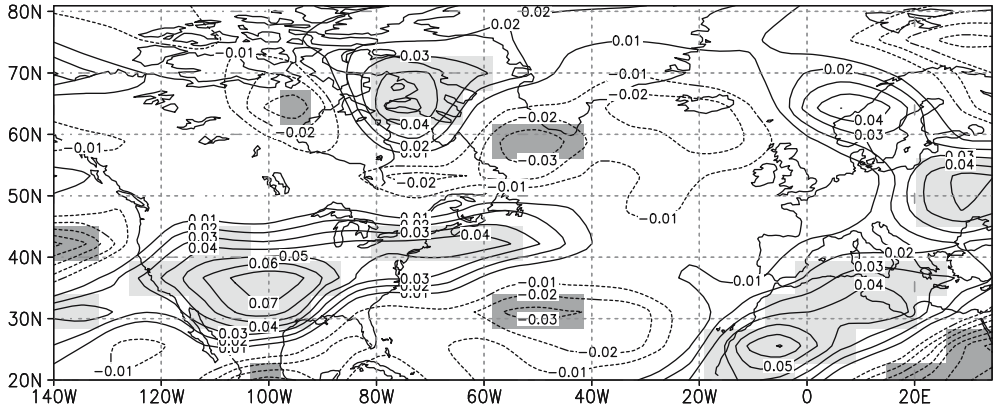

Fig. 7 Difference in the Eady index at 650 hPa between the data-assimilated simulation and the control simulation. Data are for the DJF season and averaged over the length of the simulations. The light (dark) gray areas are increases (decreases) in the Eady index which are significant at the 95% level

frequent in the DA simulation compared to the control simulation. South of 47.8°N at this longitude, no large changes in the probability distribution between the runs in found.

Baroclinic instabilities are at the origin of mid-latitude weather systems, and an appropriate measure for baroclinicity is the Eady growth rate maximum (Hoskins and Valdes 1990), or Eady index. Figure 7 shows the difference in the Eady index averaged over the simulations for the DJF season, and indicates enhanced baroclinicity in the DA simulation along the eastern seaboard of the US, roughly between Cape Hatteras and Newfoundland. This maximum extends into the North Atlantic and into the American continent to have a maximum over the Texas/Oklahoma region.

In the northwestern North Atlantic, off the eastern seaboard of Canada and the US, a large positive SST anomaly is found between circa 40°N and 50°N (Fig. 10). Continental temperatures at this latitude were slightly lower, but this change is not statistically significant. These are favourable baroclinic conditions for cyclogenesis, which is reflected in the anomalously high Eady index. The band of increased cyclonic activity found in Fig. 5 roughly between 30°N and 42°N is partly situated over the area with increased baroclinicity, suggesting that the dominant cause of the observed increase in cyclonic activity was the enhanced baroclinicity at the coast during 'Dalton Minimum' conditions. However, to a large extent the increase in cyclone activity came about as a result of redistribution of cyclone activity rather than increased cyclogenesis. A comparison of Figs. 5 and 7 shows that areas with increased baroclinicity, like near 45°N, do lead to an increase in cyclone activity, but this fails to be statistically significant.

Another maximum in baroclinicity at 650 hPa is found over the Labrador Sea/Baffin Bay area, with a maximum over Hudson Strait. The increase in baroclinicity can be related to anomalies in snow cover over Canada and over the sea ice in the Baffin Bay. The anomalous low pressure area situated over eastern Canada (Fig. 4) advects relatively moist air along the Atlantic seaboard northward. This results in a significant increase in snow cover at the northern and northeastern flanks of this low pressure area. At the southwestern, southern, and southeastern flanks a decrease in snow cover is found; the supply of moist oceanic air to these parts has decreased in favour of advection of dry continental air. The change in snow cover leads to a change in surface albedo, with its largest gradient over the Hudson Strait, leading to favourably conditions for developing baroclinic instabilities.

A small increase in sea-ice cover is found in the southeastern Labrador Sea (≈61°N–69°N, ≈59°W–51°W). The sea-ice fraction increases with 1–5% in that area. With the southward expanding sea-ice cover, the ice-edge baroclinicity could also be found at more southerly latitudes, where cold air flows over the sea-ice into the open water, leading to a rapid deepening of cyclones. Although the cyclone activity is pushed southward in this area (Fig. 5), we do not see an increase in baroclinicity in the Eady index at 650 hPa (Fig. 7).

Oceanic response

Meridional geostrophic water transport is related to the curl of the wind stress τ by the Sverdrup principle (Pedlosky 1987). The anomalous $\nabla \times \tau$, significant at the 95% level, is shown in Fig. 8. A large area in the northeastern North Atlantic has a negative $\nabla \times \tau$, indicating anomalous southward Sverdrup transport. A diagram of the change in vectorial surface velocity between the DA and control run (over the DJF season) shows, consistent with the Sverdrup principle, anomalous southward volume transport in the GIN Sea, along the Norwegian coast and the northern edge of the North Sea, extending to the Atlantic side of Scotland and Ireland (Fig. 9). The anomalous southward flow in the eastern GIN-Sea decreases the northward flow of relatively warm water, making the North Sea and the Norwegian Sea and the Atlantic surrounding the British Isles colder than in the control simulation (Fig. 10a). The temperature decrease is significant at the 95% level. The decrease in sea surface temperatures due to the intrusion of cold waters in the coastal waters of north

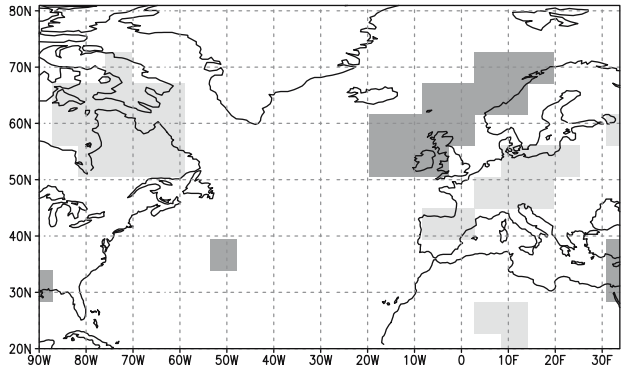

Fig. 8 Anomalous curl of the windstress τ for the DJF season, averaged over the length of the data-assimilated simulation. Meridional flow is related to the curl of the wind stress by the Sverdrup relation: $v = \nabla \times \tau$. The dark gray areas have negative wind stress curl, the light gray areas have a positive wind stress curl. The results are significant at the 95% level

western Europe is persistent into the summer season (Fig. 10b).

A weakening of the subpolar and the subtropical gyre is also seen in Fig. 9 and, connected with this, a decrease in the strength of the Gulf Stream. This decrease in significant at the 95% level. A repositioning of the Gulf Stream/North Atlantic Current system is not observed in the DA simulation. A change in the position of the isoline $\nabla \times \tau = 0$, which would be indicative of a repositioning of the polar front, is not observed either.

Interestingly, although the strength of the meridional overturning circulation decreases in the course of the DA simulation, this change fails to be statistically significant at the 95% level. This suggests that the meridional overturning circulation does not contribute to the cooling of the European continent under 'Dalton Minimum' conditions. However, the meridional overturning system does respond to the changes in the northern North Atlantic ocean. The model's main convection site in the northeastern North Atlantic shifts to a more southerly latitude (not shown). Convection in the Labrador Sea and south of Iceland, the model's other convection sites, are highly variable quantities in the simulation and no evidence is found of convective activity shifting its emphasis from the northeastern North Atlantic to the Labrador Sea or south of Iceland.

Despite the decrease in the meridional overturning circulation not being statistically significant, we do find a statistically significant (95%) decrease in oceanic meridional heat transport at 35°N (Fig. 12) and at latitudes south and north of this. This must be related to a weakening of the subpolar and the subtropical gyres (Fig. 9). The yearly-averaged oceanic meridional heat transport at 35°N in the control simulation is 0.64 PW.

In the northwestern North Atlantic, off the eastern seaboard of Canada and the US, a large positive temperature anomaly of the slope water is found. The area north of the Gulf Stream is usually very cold due to advection of cold waters from the Labrador Sea, flowing south along the eastern coasts of Canada and the US. The anomalous circulation in the DA simulation during the DJF season (Fig. 9) indicates that the southward advection of water from the Labrador Sea is decreased,

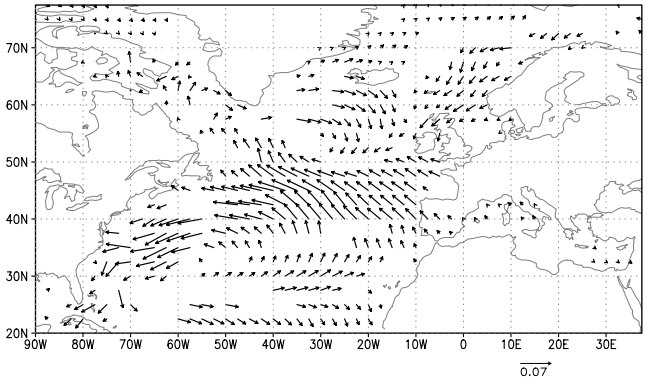

Fig. 9 Anomalous DJF surface circulation between the data-assimilated and the control simulation. The data-assimilated simulation is characterized by an anomalous southward flow in the eastern part of the GIN Sea and a weaker Gulf Stream and subtropical and subpolar gyre circulation

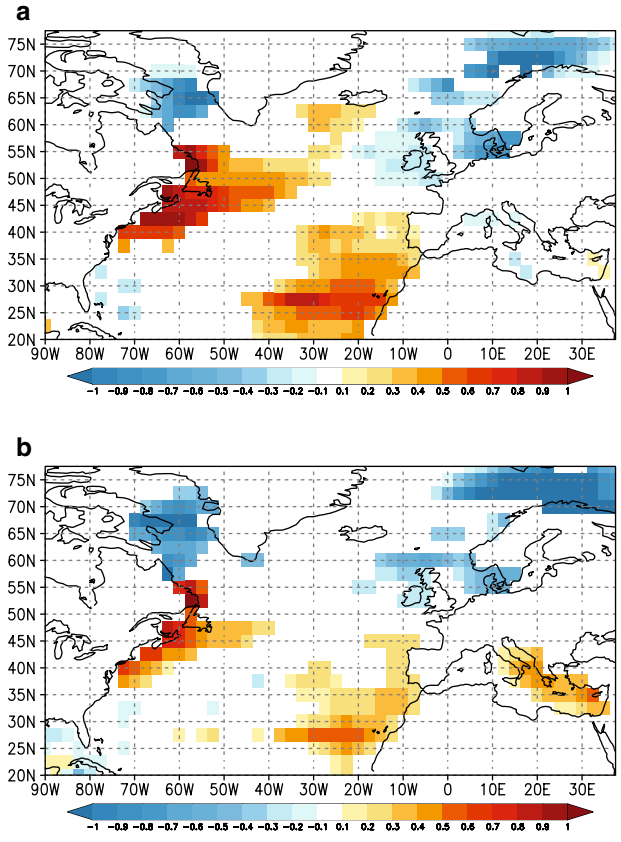

Fig. 10 Difference Sea Surface Temperature (SST) between the data assimilated and the control run for the DJF (fig. a) and the JJA season (fig. b), averaged over the latter 15 years of the data-assimilated simulation. Temperature differences which are not statistically significant at the 95% level are not drawn

with anomalous westward advection of relatively warm waters into the slope water region. This results in anomalously high SSTs, despite the decrease in oceanic meridional heat transport. The change in the surface temperatures are significant at the 95% level, but the anomalous meridional surface currents and anomalous windstress curl are only significant at the 90% level. Note however, that the Gulf Stream in this model fails to separate from the coast and hugs the coast beyond Cape Hatteras, a common feature of coarse resolution ocean models. This suggests that the warming in the northwestern North Atlantic may be an unrealistic, model-related feature.

Temperature response

The DA simulation shows dramatic changes in 2m temperatures over the European continent compared to the control simulation (Fig. 13). In the winter (DJF) season, temperatures are more than 3°C colder over northern Scandinavia to around 0.5°C colder over Spain. A positive anomaly can be found over the north-western North Atlantic, with a maximum over the Labrador Sea, although this is limited in spatial extent. In the summer (JJA) season, temperatures are lower in the eastern half of the North Atlantic with minima of circa −0.9° C over the UK. The zero degree isotherm runs from south of Spain, over central Europe and Denmark to Norway. Positive anomalies are found over Poland/western Russia and over the north-eastern American continent.

Much of the winter temperature response on the European continent can be explained by an advective effect of the anomalous atmospheric circulation, transporting cold air from the Arctic over Scandinavia into Europe. The decrease in SSTs in the northeastern North Atlantic and around the British Isles of 0.25–0.75° C (Fig. 10) contributes to this. In a narrow zone extending from the North Sea over Scotland to Iceland a negative anomaly in the latent heat flux of −4 to −8 Wm^{-2} is found (Fig. 11a, heat flux changes significant at the 90% level). Changes in the winter sensible heat flux fail to be significant at the 90% level. The temperature increase in the Labrador area is related to the transport of relatively warm air from the central North Atlantic into this area.

In summer however, the model atmosphere is unconstrained by DA. The observed temperature anomaly over western Europe is partly due to a lowering of the SSTs in the north-eastern North Atlantic (Fig. 11). The summer sensible heat flux anomaly is negative over large areas of the northern North Atlantic including an area from the North Sea to the waters surrounding the British Isles extending to Iceland. The anomaly is ca. −3 to −8 Wm^{-2} (Fig. 11b, significant at the 90% level). The sign of the heat flux anomaly is such that in the northeast Atlantic we find excessive cooling of the air masses while in transit over the ocean. Consequently, atmospheric circulation from a westerly to northerly direction advects anomalously cool air onto the continent, providing strong oceanographic support for maintaining low summer temperatures. Changes in the latent heat flux over the ocean for the summer season

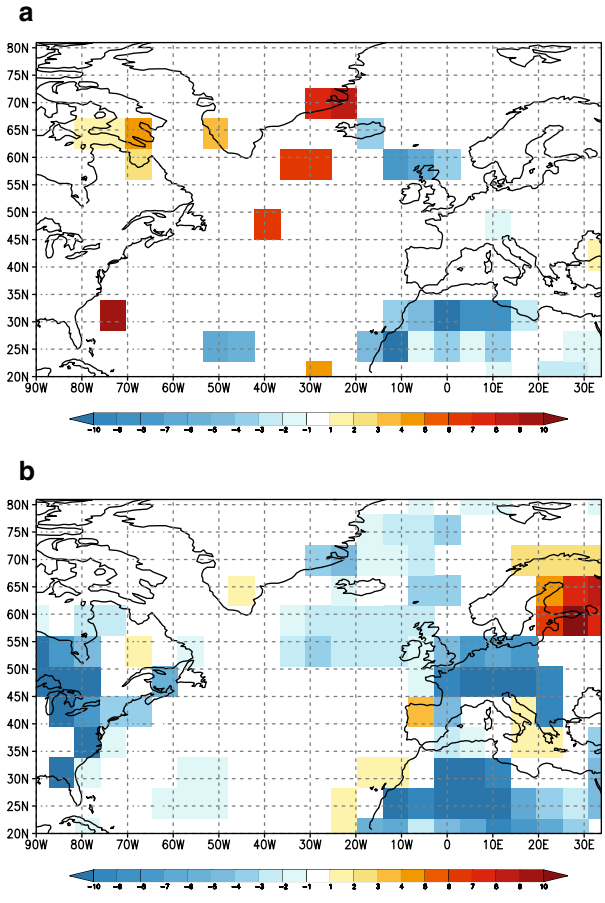

Fig. 11 Latent heat flux for the winter (DJF) (a) and sensible heat flux for the summer season (JJA) (b). Time averaged differences between the data assimilated and the control run are shown in W m^{-2}. Heat flux differences which are not statistically significant at the 90% level are not drawn

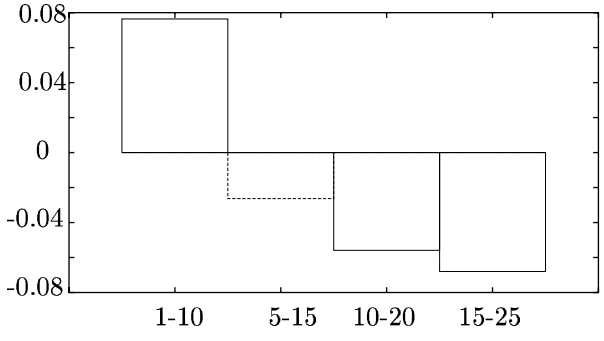

Fig. 12 Anomalous yearly-averaged meridional heat transport in the Atlantic at 35°N as a function of 10-year intervals in PW. Oceanic heat transport reduces in the course of the data-assimilated simulation, where the dashed box fails to be significant at the 95% level

were very modest or failed to be significant. A rough back-of-the-envelope calculation shows that the influence of the anomalous heat flux as an explanation for the cooling near the British Isles is quite reasonable. This calculation has earlier been used by Namias (1963). If the anomalous heat flux was used to heat a column of air of 1 km, and

$$\frac{\Delta T}{\Delta t} = \frac{\Delta Q}{c_p \rho h}$$

where ΔQ is the anomalous heat flux per day, c_p the specific heat of air (1.005 kJ kg^{-1} K^{-1}), ρ the density of air (1.205 kg m^{-3}), h the height of the column of air and ΔT the temperature change, then the anomalous heat flux would relate to a cooling of ca. 0.2–0.6° C per day. Estimating the transit time at 1 day, we have a figure that is comparable to the observed cooling in the model around the British Isles.

Over land, however, large negative anomalies in latent heat flux exist. This is related to a strong negative anomaly in bottom moisture during the simulated Dalton Minimum period in northwestern Europe, related in its turn to a decrease in (winter and summer) precipitation (not shown). Drier summer conditions on the European continent, related to the reduction in bottom moisture, relaxes a constraint on the rise of temperature by reducing the amount of evaporation. The positive 2m temperature anomaly in Central and Eastern Europe is related to this. A similar reduction in bottom moisture by a reduction in summer and winter precipitation, accounts for the warmer summer temperatures in the northeastern USA.

However, the decrease in summer temperatures over the western fringes of the European continent cannot be explained by a decrease in SSTs and the sensible heat flux only. The decrease in SSTs near the British Isles is circa 0.25–0.5°C (Fig. 11b) while the decrease over the UK is nearer 0.9°C. We relate this discrepancy to a weak anomalous atmospheric circulation with a weak high between Iceland and Ireland and a weak low over northern Poland. This anomalous circulation advects cold air from higher latitudes to western Europe and exposes these airmasses to the negative anomaly in the sensible heat flux. The shape of the 2m temperature anomaly over the North Atlantic (Fig. 13b), with the strongest cooling at high latitudes, requires that explanation. The circulation anomaly is significant at the 90% level. The position of the low is very close to the high anomalous temperatures at eastern Poland/western Russia and we suspect the low to be a secondary phenomenon.

Discussion

The assimilated changes in the mean of the atmospheric circulation of the North Atlantic sector have a direct impact on the oceanic winddriven circulation and generated anomalous southward geostrophic Sverdrup transport. The decrease in sea surface temperatures in the northeastern North Atlantic, including the North Sea and the Norwegian Sea associated with this compares well with a reconstruction of SSTs in the summer of 1789 on the basis of results of an expedition (Lamb 1979, Fig. 11), showing a decrease of 0.5–1.0°C in the waters invading the northern North Atlantic and the North Sea. Also, a recent reconstruction of paleotemperatures at the Norwegian coast (Kristensen et al. 2004) showed cooler conditions during the 1790–1820 period of ca. 2.2°C at southwestern Norway to about 0.6°C at ca. 66°N and 0.2°C somewhat off-shore at ca. 64°N. With the exception of the first, the cooling of SSTs found in the simulation is about the same.

Koslowski and Glaser (1999) have reconstructed the ice winter severity in the western Baltic and found that in the period AD 1790–1820 the ice winter index was ca. 0.8 while the average value for the 1501–1995 period was well below that at 0.546. The simulated winter SSTs in this area for this period were about 1.1°C lower than in the control simulation, which tends to be supported by the Koslowski and Glaser study. However, no statistical significant changes in sea-ice cover could be detected in the simulation. We relate this to the fact that the SSTs in the ocean model are generally too high compared to modern observations (Opsteegh et al. 1998).

Although a reduction in the meridional overturning circulation (MOC) is observed in this simulation, this reduction fails to be statistically significant, and cannot serve as an explanation for the magnitude of the decrease in sea surface temperatures. Apparently, a decrease in temperatures over western Europe resulting from ocean-atmosphere interaction, where the atmospheric circulation is consistent with reconstructions of the circulation under Dalton Minimum conditions, does *not* involve the MOC. The role of the overturning during the cooler periods within the Little Ice Age is, from the marine geological perspective, controversial. Some data suggest a slackened meridional overturning (Broecker 2000; Bianchi and McCave 1999), while Keigwin and Boyle (2000) argue that the evidence is inconclusive. The apparent lack of a participating MOC in the deterioration of the European temperatures during the Dalton Minimum as observed in this study puts this discussion in a different perspective.

One difference between Bjerknes' hypothesis and the simulation of possible Dalton Minimum climate discussed in this study is the lack of a repositioning of the Gulf Stream to a more zonal orientation and the associated changes in subtropical sea surface temperatures. The response of the Gulf Stream in our simulation is characterized as a simple decrease in strength. The limited southward extent of the anomalous minimum in the atmospheric streamfunction located over southeastern Canada (Fig. 4) which is associated with the deep trough in the streamfunction, may be related to the absence of a repositioning of the Gulf Stream. The anomalous northward Sverdrup flow just off the eastern seaboard of the US is not apparent in the DA simulation (Fig. 8) and

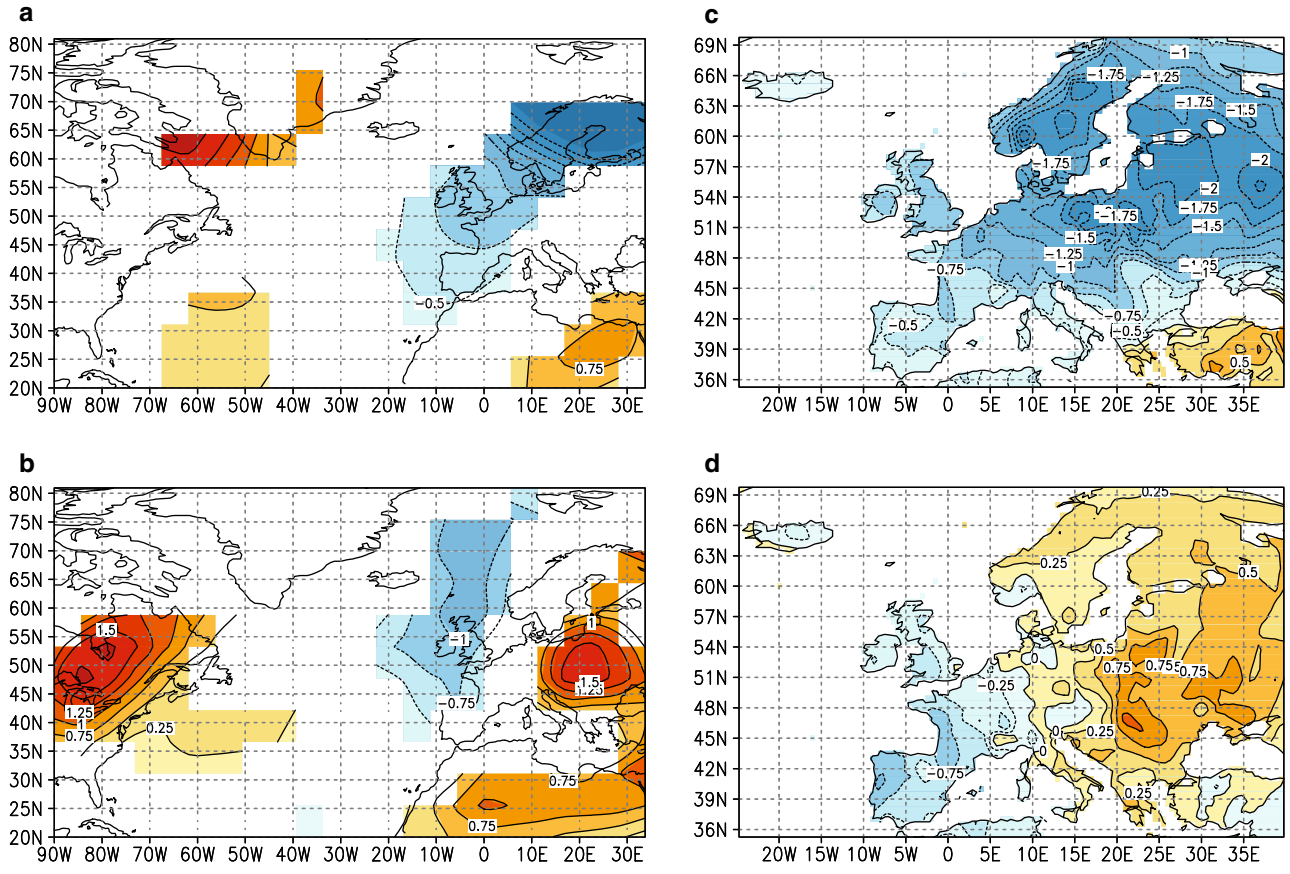

Fig. 13 Difference in 2 meter temperature, averaged over 25 year, for the winter (DJF) season (fig. a) and the summer (JJA) season (fig. b) between the data-assimilated and the control run. In both seasons, north-western Europe is under the data-assimilated run colder than in the control run. All temperature changes shown are statistically significant at the 95% level. Figures c and d show the difference in reconstructed surface air temperature for the period 1790-1820 AD with respect to 1971-2000, for the winter (DJF) season (fig. c) and the summer (JJA) season (fig. d). Reconstructed temperatures are from Luterbacher et al. (2004)

was hypothesized by Bjerknes to bring about both this repositioning and an increase in Sargasso Sea temperatures. A possible reason for the observed warming of the waters off Nova Scotia rather than the hypothesized cooling may be the poor horizontal resolution of the ocean model and the associated poorly represented Gulf Stream dynamics and a Gulf Stream position which is not supported by reality.

Interestingly, the simulation of northwest Atlantic SSTs tend to agree with a SST reconstruction based on proxy evidence (Keigwin and Pickart 1999) which suggests *warmer* slope water during the sixteenth to nineteenth centuries. The simultaneous cooling of the Sargasso Sea waters, as suggested by analysis of marine sediments from the Bermuda Rise (Keigwin 1996) is not observed in the simulation.

Based on marine sediment analysis, Jennings et al. (2001) concluded that the period under investigation falls in the period of severe sea-ice conditions around Iceland. Persistently severe sea-ice conditions, or even an increased severity around Iceland, are not reproduced in the simulation. Nevertheless, years with excessive sea-ice around Iceland's northern and southern coasts are present in the simulation, but the sea-ice extent around Iceland is highly variable in the simulation. This leaves finding a statistically significant change or trend in sea-ice unreliable.

An aspect of change in the simulation of possible Dalton Minimum climate is that the Atlantic storm tracks showed a higher variability in its position. Both north and south of the model's control climate are areas of enhanced cyclonic activity. The strength of the cyclones in mid-latitudes changed too; a higher occurrence probability of the strongest cyclones was observed under Dalton Minimum atmospheric circulation conditions. This is consistent with the notion that some storms in the colder periods of the Little Ice Age period exceeded twentieth century extremes in intensity (Lamb 1979; Glaser 2001), at least for the European mid-latitudes. To a large extend this increase in cyclone frequency can be related to a redistribution of cyclone activity rather than being attributed solely to increased baroclinicty. However, areas with increased baroclinicity are found just off the northeastern Atlantic seaboard of the US and in the Baffin Bay/Labrador Sea area. The former increase is associated with an increase in land-sea temperature contrast. The latter increase is associated with the emergence of a steep gradient in surface albedo over the

Hudson Strait area which is related to changes in the snow cover.

The other aspect of Bjerknes' theory which seem to be absent in this simulation is an increase in the steering of cyclones into the northwest Atlantic. Bjerknes suggested that the favourable baroclinic conditions along the eastern seaboard of the US would lead to a stronger deepening of cyclones, leading to a situation where extensive lows would stagnate in the Newfoundland-Labrador area rather than proceeding toward Iceland. This would account for the anomalously deep pressure trough in the SLP reconstruction at this location and could then be evidence of an ocean-atmosphere feed back, which could sustain the atmospheric circulation from which is was generated. The relevance of this suggestion for climate in the North Atlantic sector was demonstrated in a study (Dickson and Namias 1976) where months of extreme winter cold in the southeastern US showed an increase in baroclinicity at the Atlantic seaboard and an increase in cyclonic activity in the northwest Atlantic. No increase of stagnating cyclones in the Newfoundland-Labrador area, originating along the Atlantic seaboard is observed in this study. This suggests that the feedback hypothesized above was not present in the simulation. The absence of steering lows from the Atlantic seaboard to the Labrador area may be due to the low resolution of the atmospheric model (T21).

The North Atlantic Oscillation (NAO) is the most dominant mode of variability in the winter atmospheric circulation over the North Atlantic sector (Hurrel 1995). Although the 1790–1820 reconstructed pressure anomaly (Fig. 1d) with respect to the 1971–2000 SLP field, is not similar to the classical NAO-pattern, it does project on this pattern having a pressure anomaly between Iceland and the Azores. The NAO-index over the data-assimilated simulation is slightly negative at −0.08. A reconstructed NAO-index based on instrumental and documentary data (Luterbacher et al. 2002a) is averaged over the 1790–1820 period is more strongly negative at −0.14. The weakening and southwest ward shift in the positive anomaly over Iceland in the simulation compared to the reconstruction (Fig. 4) must add to this discrepancy.

Finally, the simulation shows a strong decrease of surface air temperatures in western Europe for both the winter and the summer season. For central Europe, the winter temperature signal fails to be significant while in summer temperatures increase in central Europe. We have compared the simulated surface air temperature anomalies with a recent reconstruction of surface air temperatures (Luterbacher et al. 2004) (Fig. 13). The two patterns show a remarkable similarity. Both patterns show strong cooling in the winter western European continent which gradually decreases southward. The strength of the cooling in the simulation also compares favourably to the reconstruction. In summer both the simulation and the reconstruction show a dipole-like structure with cooling on the western fringes of the European continent, extending as far south as Spain, and a warming in central Europe. However, the warming in central Europe is overestimated by about 0.25–0.5°C, while the cooling over the British Isles is overestimated with ca. 0.5°C. We relate the latter overestimation to a weak anomalous atmospheric circulation with a low over northern Poland and a high between Iceland and Ireland, advecting cold air southward over the British Isles. Note that the decrease in summer sea surface temperatures around the British Isles is around 0.25–0.5°C and thus comparable to the decrease observed in the reconstructed temperature record.

A tentative explanation for the absence of strong central European winter cooling in the simulation is related to the absence of a parametrization of the effects of the strong volcanic outbursts and the reduction in solar activity on climate as they occurred during the 1790–1820 period. The reduction in solar irradiance which is associated with these events (Weber et al. 2004) will have largest impact on areas which are characterized by a land climate like the central European region, rather than areas with a maritime climate.

Summary and conclusions

Bjerknes' theory on the coldness in northwestern Europe during the period AD 1780–1820 elegantly addresses a number of facts that call for explanation. The validity of this theory has been investigated using a climate model of intermediate complexity. Bjerknes' hypothesis hinges on anomalous ocean-atmosphere interaction, and he based it on a reconstruction of sea level pressure over the period 1790–1829; a period we now call the Dalton Minimum. By basically using the Sverdrup relation, which relates meridional geostrophic water transport to the curl of the wind stress, he conjectured both a change in ocean surface circulation and an associated change in SSTs. Subsequently, these changes in the ocean climate were hypothesized to feed back on two aspects of the climate system. (1) An increase in oceanic surface temperature in the western Sargasso Sea led to an increase in baroclinicity near the eastern seaboard of the North American continent, and consequently led to an intensification of cyclogenesis, and (2) a decrease in oceanic temperature in the northeast Atlantic Ocean led to a cooling of the European continent.

Central in this study is the use of a DA technique which stems from numerical weather prediction theory. The application of this technique to paleoclimatology is new. In this technique, a perturbation to the forcing terms of the atmospheric equations of motion is computed, which optimally leads the atmospheric model to a specified pattern. These perturbations are referred to as forcing singular vectors (Barkmeijer et al. 2003). With this technique we analyse ocean-atmosphere interaction under possible Dalton Minimum conditions. A reconstruction of atmospheric circulation averaged over the years AD 1790–1820, over the Atlantic sector, is assimilated in the model. This results in a simulation of

global climate which is, over the Atlantic sector, consistent with this reconstruction while storm track dynamics and synoptic scale atmospheric variability are not suppressed. This demonstrates the viability of the forcing singular vectors technique in assimilating large-scale patterns in general circulation models. The ability to assimilate large-scale patterns of atmospheric circulation in a climate model without suppressing any internal atmospheric variability, leaves the atmosphere free to interact realistically and in a dynamically consistent manner with the other climate components. This provides evidence that this technique can be applied to the investigation of other problems in paleoclimatology.

In this study we have shown that a change in atmospheric winter circulation, as one associated with Dalton Minimum conditions, can indeed lead to a reduction in both winter and summer temperatures over the (western) European continent and involves a change in ocean surface temperatures in the north-east North Atlantic due to ocean-atmosphere feed back processes. The temperature reduction as simulated by this model under Dalton Minimum atmospheric circulation conditions near the UK would be comparable to reconstructed temperatures for this period, albeit with some overestimation of the summer cooling. From this we conclude that the anomalous winter atmospheric circulation can explain the largest part of the observed winter cooling in north-western Europe. The decrease in temperatures of the waters surrounding the British Isles combined with a weak anomalous circulation over the northern North Atlantic explains the summer cooling of the western fringes of the European continent.

This study indicates that under Dalton Minimum atmospheric circulation conditions there was enhanced cyclonic activity both south and north of the modern storm track position. From this we conclude a higher variability in the position of the North Atlantic storm-tracks in the simulation. Furthermore, the strength of the cyclones in mid-latitudes changed; a higher occurrence probability at the European mid-latitudes of the strongest cyclones was observed under Dalton Minimum atmospheric circulation conditions. To a large extend this increase in cyclone frequency can be related to a redistribution of cyclone activity rather than being attributed solely to increased baroclinicty. However, areas with increased baroclinicity are found just off the northeastern Atlantic seaboard of the US and in the Baffin Bay/Labrador Sea area.

The aspects of Bjerknes' theory that could not be affirmed relate to the changes in the Atlantic's subtropical SSTs that Bjerknes envisioned and to an absence of stagnating low-pressure systems in the Labrador Sea area.

In closing it must be readily admitted that many aspects of climatic change associated with the European Dalton Minimum period are not analyzed in detail in this study, like changes in precipitation and the change of glacier length of Europe's glaciers. However, this study demonstrates the plausibility of Bjerknes' (1965) hypothesis and the relevance of ocean-atmosphere interaction for explaining some aspects of the European Dalton Minimum climatic anomaly.

Acknowledgements NCEP Reanalysis data provided by the NOAA-CIRES Climate Diagnostics Center, Boulder, Colorado, USA, from their Web site at http://www.cdc.noaa.gov. The Luterbacher et al. (2002) SLP reconstruction is available from IGBP PAGES/World Data Center A for Paleoclimatology, NOAA/NGDC Paleoclimatology Program, Boulder CO, USA. J. Luterbacher is thanked for making available the Luterbacher et al. (2004) European temperature reconstruction and G.J. van Oldenburgh for making available the KNMI Climate Explorer (http://www.climexp.nl). Thanks go to S.L. Weber, K.R. Briffa, T.J. Osborn, J. Luterbacher and two anonymous referees for carefully reviewing this paper. GvdS is funded by the Natural Environment Research Council (NERC) through the RAPID Climate Change programme.

Appendix

Forcing singular vectors

An introduction to forcing singular vectors applied to the context of this study follows here. A more extensive account is given by Barkmeijer et al. (2003), where the application used in this study is termed 'forced sensitivity calculations'.

Write the climate model in the following abstract form,

$$\frac{dx}{dt} = G(x), \tag{3}$$

with **x** the vector containing all prognostic variables of the model and G(**x**) the model formulation. In numerical weather prediction models, the forecast quality will depend on e.g. the parametrization of physical processes in the model formulation, which motivates studying the model response to small perturbations of the model tendencies. Here, we assume that the (external and/or internal) forcings which gave rise to a historic atmospheric state, anomalous to a modern climatology, can be regarded as a perturbation **f** of the model tendencies (whose spatial pattern and amplitude is kept constant in time). The linear evolution equation of this anomaly in the atmospheric state ε satisfies:

$$\frac{d\varepsilon}{dt} = \mathbf{L}\varepsilon + \mathbf{f}, \tag{4}$$

where **L** denotes the time dependent Jacobian of G, evaluated along a solution of equation (Eq. 3). Solutions of equation (Eq. 4) take the form:

$$\varepsilon(T) = \mathbf{M}(0,T)\varepsilon(0) + \int_0^T M(s,T)\mathbf{f}ds, \tag{5}$$

where **M**(s, T) is the propagator from time s to time T of equation (Eq. 4) without forcing: **f** = 0. For an arbitrary forcing **f**, the vector **y** = $\mathscr{M}$**f**, where

$$\mathscr{M} = \int_0^T \mathbf{M}(s,T)ds, \tag{6}$$

is simply determined by integrating (Eq. 4) to time $t = T$ with initial condition $\varepsilon(0) = 0$.

The forcing perturbation is now determined by minimization of the cost function

$$J(f) = |P(\mathscr{M}\mathbf{F} - \psi| \tag{7}$$

where ψ is the target pattern and P is a projection operator onto the extra-tropical North Atlantic sector (taken to be bounded by 90°W–40°E, 15°N–90°N). The gradient of $J(f)$, required in the quasi-Newton conjugate gradient method (NAG's E04DGF), is:

$$\nabla J = 2\mathscr{M} * P * P(\mathscr{M}f - \psi) \tag{8}$$

To derive the adjoint of $\mathscr{M}$ it is instructive to write (Eq. 4) as:

$$\frac{d}{dt}\begin{pmatrix}\varepsilon\\ \mathbf{f}\end{pmatrix} = \begin{pmatrix}\mathbf{L} & \mathbf{I}\\ 0 & 0\end{pmatrix}\begin{pmatrix}\varepsilon\\ \mathbf{f}\end{pmatrix}, \tag{9}$$

where $\mathbf{I}$ and $\mathbf{0}$ are the identity and zero operator respectively. The adjoint of (Eq. 9) is:

$$-\frac{d}{dt}\begin{pmatrix}\hat{\varepsilon}\\ \hat{\mathbf{f}}\end{pmatrix} = \begin{pmatrix}\mathbf{L}* & \mathbf{I}\\ 0 & 0\end{pmatrix}\begin{pmatrix}\hat{\varepsilon}\\ \hat{\mathbf{f}}\end{pmatrix}. \tag{10}$$

By writing (Eq. 10) as a coupled system:

$$-\frac{d}{dt}\hat{\varepsilon} = \mathbf{L} * \hat{\varepsilon} \tag{11}$$

$$-\frac{d}{dt}\hat{\mathbf{f}} = \hat{\varepsilon} \tag{12}$$

it follows how to determine $\mathscr{M} * \mathbf{y}$ for a given input vector $\mathbf{y}$. First: integrate the regular adjoint model as given by equation (Eq. 11) backward in time $t = T$ to time $t = 0$, with $\hat{\varepsilon}(T) = \mathbf{y}$. Second: integrate equation (Eq. 12) backward in time from time $t = T$ using the intermediate fields of the adjoint integration (Eq. 11) as tendencies for the corresponding time step and $\hat{\mathbf{f}}(T) = 0$. Integrating to time $t = 0$ yields

$$\mathscr{M} * \mathbf{y} = \hat{\mathbf{f}}(0)$$

References

Barkmeijer J, Houtekamer P, Wang X (1993) Validation of a skill prediction model. Tellus 45A:424–434

Barkmeijer J, Iversen T, Palmer TN (2003) Forcing singular vectors and other sensitive model structures. Quart J R Met Soc 129:2401–2423

Bianchi GG, McCave IN (1999) Holocene periodicity in North Atlantic climate and deep-ocean flow south of Iceland. Nature 397:515–517

Bjerknes J (1965) Atmosphere-ocean interaction during the 'Little Ice Age'. In: WMO-IUGG Symposium on Research and Development Aspects of Longe-Range Forecasting WMO-No. 162. TP. 79, pages 77–88 Technical Note No. 66

Broecker WS (2000) Was a change in thermohaline circulation responsible for the Little Ice Age?. Proc Natl Acad Sci USA 97:1339–1342

Crowley TJ (2000) Causes of Climate Change Over the Past 1000 Years. Science 289:270–277

Dickson RR, Namias J (1976) North American Influences on the Circulation and Climate of the North Atlantic Sector. Mon. Wea. Rev. 104:1255–1265

Glaser R (2001) Klimageschichte Mitteleuropas: 1000 Jahre Wetter, Klima, Katastrophen. Primus Verlag

Goosse H, Fichefet T (1999) Importance of ice-ocean interactions for the global ocean circulation: a model study. J Geophys Res (Oceans) 104:23337–23355

Goosse H, Deleersnijder E, Fichefet T, England MH (1999) Sensitivity of a global ocean-sea ice model to the parametrization of vertical mixing. J Geophys Res (Oceans) 104:13681–13695

Grove J (1988) The Little Ice Age. Methuen and Co, London

Haigh JD (1996) The Impact of Solar Variability on Climate. Science 272:981–984

Hale E (1833) A Meteorological Journal from the Year 1786 to the Year 1829, inclusive, by Edward A. Holyoke, M.D., A.A.S. Mem. Amer Acad Arts Sci. 1:107–216

Harington CR editor (1992) The Year Without a Summer?. World climate in 1816. Canadian Museum of Nature, Ottawa Canada

Hartmann DL, Wallace JM, Limpasuvan V, Thompson DWJ, Holton JR (2000) Can ozone depletion and global warming interact to produce rapid climate change?. Proc Nat Acad Sci USA 97:1412–1417

Havens JM (1956) An Annotated Bibliography of Meteorological Observations in the United States, 1731-1818. Technical Report No. 5, Florida State University, Department of Meteorology. Prepared under project NR-082-071, contract NONR-1600(00) with the Office of Naval Research

Hoskins BJ, Hodges KI (2002) New Perspectives on the Northern Hemisphere Winter Storm Tracks. J Atm Sci 59:1041–1061

Hoskins BJ, Valdes PJ (1990) On the Existence of Storm-Tracks. J Atm Sci 47:1854–1864

Hurrel JW (1995) Decadal Trends in the North Atlantic Oscillation: Regional Temperatures and Precipitation. Science 269:676–679

IPCC (2001) Climate Change 2001: The Scientific Basis. Contribution of Working Group I to the third Assessment Report of the Intergovernmental Panel on Climate Change. Cambridge University Press. Houghton JT et al. (eds.)

Jennings AE, Hagen S, Hardardottir J, Stein R, Ogilvie AEJ, Jonsdottir I (2001) Oceanographic change and terrestrial human impacts in a post A.D. 1400 sediment record from the southwest Iceland shelf. Climatic Change 48:83–100

Jones PD, Mann ME (2004) Climate Over Past Millenia. Rev. Geophys. 42:RG2002 doi:10.1029/2003RG000143

Jones JM, Widmann M (2004) Reconstructing large-scale variability from palaeoclimatic evidence by means of Data Assimilation Through Upscaling and Nudging (DATUN). In: Fischer H, Kumke T, Lohmann G, Flöser G, Miller H, von Storch H, Negendank JFW (eds) The KIHZ project: towards a synthesis of Holocene proxy data and climate models, pages 171–193 Springer Verlag, Berlin - Heidelberg - New York

Keigwin LD (1996) The Little Ice Age and Medieval Warm Period in the Sargasso Sea. Science 274:1504–1508

Keigwin LD, Boyle EA (2000) Detecting Holocene changes in thermohaline circulation. Proc Nat Acad Sci USA 97:1343–1346

Keigwin LD, Pickart RS (1999) Slope Water Current over the Laurentide Fan on Interannual to Millenial Time Scales. Science 286:520–523

Klitgaard-Kristensen D, Seirup HP, Haflidason H, Berstad IM (2004) Eight-hundred-year temperature variability from the Norwegian continental margin and the North Atlantic thermohaline circulation. Paleoceano. 19:PA2007 doi:10.1029/2003PA000960

Koslowski G, Glaser R (1999) Variations in recontructed ice winter severity in the western Baltic from 1501 to 1995, and their implications for the North Atlantic Oscillation. Climatic Change 41:175–191

Lacarra J, Talagrand O (1988) Short-range evolution of small perturbations in a barotropic model. Tellus 40A:81–95

Lamb HH (1979) Climatic variation and changes in the wind and ocean circulation: the Little Ice Age in the northeast Atlantic. Quaternary Res. 11:1–20

Lamb HH (1985) The Little Ice Age period and the great storms within it. In: Tooley, Sheail (eds) The Climatic Scene. Allen and Unwin, pp 104–131

Lamb HH, Johnson AI (1959) Climatic variation and observed changes in the general circulation. Part I and Part II. Geografiska Annaler 41:94–134

Luterbacher J, Xoplaki E, Dietrich D, Jones P, Davies T, Portis D, Gonzalez-Rouco J, von Storch H, Gyalistras D, Casty, C, Wanner H (2002a) Extending North Atlantic Oscillation Reconstructions Back to 1500. Atmos. Sci. Lett. 2:114–124 doi:10.1006/asle.2001.0044

Luterbacher J, Xoplaki E, Dietrich D, Rickli R, Jacobeit J, Beck C, Gyalistras D, Schmutz C, Wanner H (2002b) Reconstructions of Sea Level Pressure fields over the Eastern North Atlantic and Europe back to 1500. Climate Dyn 18:545–561

Luterbacher J, Dietrich D, Xoplaki E, Grosjean M, Wanner H (2004) European Seasonal and Annual Temperature Variability, Trends, and Extremes Since 1500. Science 303:1499–1503

Namias J (1963) Surface-atmosphere interactions as fundamental causes of drought and other climatic fluctuations. In: Sutcliffe RC (ed) Changes of Climate; Proceedings of the Rome Symposium organized by Unesco and the WMO. Unesco

Ogilvie AEJ, Jonsson T (2001) "Little Ice Age" research: A perspective from Iceland. Climatic Change 48:9–52

Opsteegh JD, Haarsma RJ, Selten FM, Kattenberg A (1998) ECBILT A dynamic alternative to mixed boundary conditions in ocean models. Tellus 50 A:348–367

Pedlosky J (1987) Geophysical Fluid Dynamics. Springer-Verlag, New York

van de Plassche O, van der Schrier G, Weber SL, Gehrels WR, Wright AJ (2003) Sea-level variability in the northwest Atlantic during the past 1500 years: A delayed response to solar forcing?. Geophys Res Lett 30(18):1921 doi:10.1029/2003GL017558

Rind D, Lean J, Healey R (1999) Simulated time-dependent climate response to solar radiative forcing since 1600. J Geophys Res (Atmospheres) 104:1973–1990

Rind D, Shindell DT, Perlwitz J, Lerner J, Lonergan P, Lean J, McLinden C (2004) The Relative Importance of Solar and Antropogenic Forcing of Climate Change between the Maunder Minimum and the Present. J Climate 17:906–929

Robertson A, Overpeck J, Rind D, Mosley-Thompson E, Zielinski G, Lean J, Koch D, Penner J, Tegen I, Healy R (2001) Hypothesized climate forcing time series for the last 500 years. J Geophys Res (Atmospheres) 106(D14):14,783–14,803

van der Schrier G, Weber SL, Drijfhout SS (2002) Sea level changes in the North Atlantic by solar forcing and internal variability. Climate Dyn. 19:435–447

Shindell DT, Schmidt GA, Mann MA, Rind D, Waple A (2001) Solar Forcing of Regional Climate Change During the Maunder Minimum. Science 294:2149–2152

Shindell DT, Schmidt GA, Miller RL, Mann ME (2003) Volcanic and Solar Forcing of Climate Change during the Preindustrial Era. J Climate 16:4094–4107

Shindell DT, Schmidt GA, Mann ME, Faluvegi G (2004) Dynamic winter climate response to large tropical volcanic eruptions since 1600. J. Geophys. Res. (Atmospheres) 109:D05104 doi:10.1029/2003JD004151

Sterl A (2001) On the impact of gap-filling algorithms om the variability patterns of reconstructed oceanic surface fields. Geophys Res Lett 28:2473–2476

von Storch H, Cubach U, González-Rouco JF, Jones JM, Voss R, Widmann M, Zorita E (2000) Combining paleoclimatic evidence and GCMs by means of data assimilation through upscaling and nudging (DATUN). In Proc. 11th Symposium on Global Change Studies, pages 1–4. AMS

Trenberth K, Paolino DA (1980) The Northern Hemisphere sea-level pressure data set: trends, errors and discontinuities. Mon Wea Rev 108:855–872

Waple AM, Mann ME, Bradley RS (2002) Long-term patterns of solar irradiance forcing in model experiments and proxy based surface temperature reconstructions. Climate Dyn 18:563–578

Weber SL, Crowley TJ, and van der Schrier G (2004) Solar irradiance forcing of centennial climate variability during the Holocene. Climate Dyn. 22:539–553 doi:10.1007/s00382-004-0396-y

Zorita E, von Storch H, Gonzalez-Rouco FJ, Cubasch U, Luterbacher J, Fischer-Bruns I, Legutke S, Schlese U (2004) Climate evolution in the last five centuries simulated by an atmosphere-ocean model: global temperatures, the North Atlantic Oscillation and the Late Maunder Minimum. Meteorol. Zeitschrift 13:271–289